HAL
archives-ouvertes.fr

On Phasor Control for Linear Time Invariant systems

Fabricio Saggin, Anton Korniienko, Gérard Scorletti

To cite this version:

Fabricio Saggin, Anton Korniienko, Gérard Scorletti. On Phasor Control for Linear Time Invariant systems. [Research Report] Ecole Centrale Lyon. 2019. hal-02068370

HAL Id: hal-02068370

https://hal.archives-ouvertes.fr/hal-02068370

Submitted on 10 Apr 2019

HAL is a multi-disciplinary open access archive for the deposit and dissemination of scientific research documents, whether they are published or not. The documents may come from teaching and research institutions in France or abroad, or from public or private research centers.

L'archive ouverte pluridisciplinaire **HAL**, est destinée au dépôt et à la diffusion de documents scientifiques de niveau recherche, publiés ou non, émanant des établissements d'enseignement et de recherche français ou étrangers, des laboratoires publics ou privés.

On the Phasor Control for Linear Time Invariant Systems

Fabrício Saggin, Anton Korniienko and Gérard Scorletti

Abstract

In some control applications, where the reference is sinusoidal, phasor-based strategies can be considered. The main advantage of these approaches is that instead of dealing with oscillating signals, one deals with constant or low-frequency signals. However, to implement this solution, several nonlinearities are included into the control loop. Then, linearization are performed around operating points to design a controller, but with no guaranties of performance. In this work, we present a "large-signal" model for the system. Then, considering ideal measurement of instantaneous amplitude and phase, we establish the correspondence between classical control architecture and a phasor-based one. Hence, we show that a controller can be designed as in a classical architecture and implemented in a phasor-based one with a simple transformation, ensuring the same performance level. However, in practical applications, the measurements of amplitude and phase are not ideal and may quickly degrade the behavior of the system. Thus, we propose a second design approach that takes these nonlinearities into account, ensuring nominal stability and performance. Examples illustrate the effectiveness of these methods.

I. Introduction

In numerous applications, the primary objective of a controller is to ensure that some process variable y follows a sinusoidal reference trajectory y_r with a given amplitude Y_r and a given frequency ω_0 (in $\mathrm{rad\,s^{-1}}$), *i.e.*, $y_r(t) = Y_r \cos(\omega_0 t)$. For instance, we can mention the control of micro gyroscopes, that shall keep a proof mass oscillating close to a resonance frequency with a controlled amplitude [1], [2].

The general practice in control engineering is to compute the control action u based on measurements of y and y_r. However, in the above applications, another control architecture is proposed. In this alternative control architecture, the control action is based on a phasor approach [3]. The phasor is often expressed by the couple made up of the amplitude and the phase shift of a given signal with respect to the reference phase $\phi_{exc}(t) = \omega_0 t$. Then, based on the measurement of the output phasor (amplitude and phase shift) and on the reference phasor, the amplitude and the phase of the control action are computed, *i.e.*, the control signal is constrained to the form

$$u(t) = U(t)\cos(\omega_0 t + \phi_u(t)). \tag{1}$$

This strategy is illustrated in Fig. 1, where G is a linear time-invariant (LTI) system. The nonlinear block p2s transforms a phasor into a modulated signal, as in (1), and s2p transforms a modulated signal into a phasor (amplitude and phase shift) with respect to $\omega_0 t$.

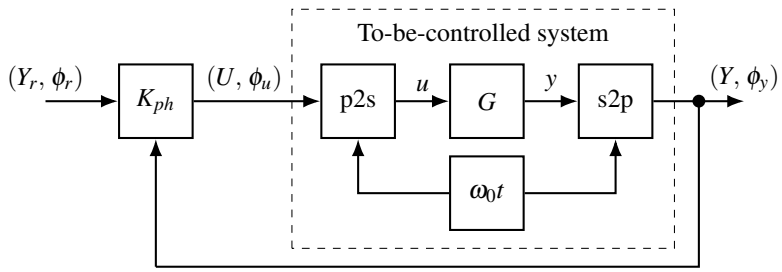

Fig. 1. Block-diagram of the phasor-based control architecture.

One advantage of this control architecture is that the phasor of the reference is a constant signal and, consequently, one can use the more classical control methods that were conceived for such type of reference signals (as PI-controllers) [1], [3]. Another advantage is that the controller works at a lower frequency than it

The authors are with the Ampère Laboratory, UMR CNRS 5005, Ecole Centrale de Lyon, Université de Lyon, Ecully, France, fabricio.saggin@ec-lyon.fr

would have in the classical architecture. However, an important drawback of that phasor control architecture is that the to-be-controlled system becomes nonlinear. Indeed, the choice to work with amplitude and phase shift representation entails these nonlinearities and makes the control design more complicated. Moreover, the conventional approach is to linearize the system around operating points [1], [3], leading to controllers whose performance cannot be guaranteed.

In this work, we show that these nonlinear operations are not required: instead of using the amplitude and phase shift representation, we can use the real and imaginary parts of the complex phasor. In this case, the system remains linear. This is one message of the present paper. Note that, even if the control architecture is fixed and imposes the use of amplitude and phase shift, we can go back in a software manner to the corresponding real and imaginary parts by inverting these nonlinearities. In this framework, we denote as s2cp the operator that, from a modulated signal, extracts the real and imaginary parts of its corresponding phasor.

In contrast to the control design methods for the classical architecture, the number of these methods for the phasor architecture remains limited. Moreover, in general, phasor-based approaches cannot guarantee the performance level of the closed-loop system. Then, another contribution of the present paper is to reveal that there is a link between the classical and the phasor architecture. This link allows transforming a controller designed for the classical architecture into a controller for the phasor architecture, yielding to the same performance level. Thus, all the linear control design methods may be transposed to the phasor approach. The only condition for this property to hold is that the phasor construction block (s2cp) is ideal.

In practice, however, nonidealities are present in the phasor construction block and may yield to a significant performance discrepancy and even instability of the closed-loop system. Another contribution of this paper is, therefore, a control design method allowing to explicitly take into account these nonidealities, ensuring the stability and an appropriate performance level.

Notation: Subscripts R and I indicate respectively the real part and imaginary part of a complex variable. The imaginary unit is denoted by j, *i.e.*, $j^2 = -1$. The variable s denotes at the same time the Laplace variable and the differential operator. I_n denotes the identity matrix of $\mathbb{R}^{n\times n}$ and $0_{n\times m}$ denotes the zero matrix of $\mathbb{R}^{n\times m}$ (subscripts are omitted if obvious from context). For two matrices A, B, $\mathrm{diag}(A,B)$ denotes $\begin{bmatrix} A & 0 \\ 0 & B \end{bmatrix}$. A^T is the transpose of A and A^* is its complex conjugate transpose. For a full column rank matrix M, $M_\perp$ denotes its orthogonal complement, *i.e.*, $M^* M_\perp = 0$ and $[M^* \; M_\perp]$ is of maximum rank. In linear matrix inequalities (LMI), $\diamond$ represents terms that can be deduced from symmetry. For a complex matrix M, $\overline{\sigma}(M)$ denotes the maximum singular value of M. The $\star$ denotes the Redheffer (star) product [4]. For a given LTI system F, $\|F\|_\infty$ denotes the H_∞-norm of F. We denote $T_{a\to b}$ the transfer from a to b. The L_2-norm of a signal v from $\mathbb{R}^+$ to $\mathbb{R}^{n_v}$ is defined as $\|v\|_2^2 = \int_0^\infty v(t)^T v(t)\mathrm{d}t$ and the set of signals for which the L_2-norm is bounded is denoted L_2. Then, the L_2-gain of an operator Σ is defined as $\|\Sigma\|_2 = \sup_{v\in L_2,\, v\neq 0} \|\Sigma v\|_2 / \|v\|_2$.

II. Phasor control problem

Let us consider the linear time invariant plant

$$G: \begin{cases} \dot{x}(t) = Ax(t) + Bu(t) \\ y(t) = Cx(t) + Du(t) \end{cases} \tag{2}$$

with $x(t) \in \mathbb{R}^n$, $u(t) \in \mathbb{R}^{n_u}$, $y(t) \in \mathbb{R}^{n_y}$, and real matrices A, B, C and D of appropriate dimensions. The original control objective is to compute u in order that y tracks a sinusoidal reference y_r at frequency ω_0 and/or reject sinusoidal disturbances at the same frequency.

In Automatic control, this problem is usually solved by computing a linear time invariant control law using *e.g.* the H_∞ approach (see [4]), which computes u from the measurement of y and y_r. In the sequel, this approach is referred to as the **direct control problem**.

Nevertheless, for this particular problem, an alternative approach, named the **phasor control problem**, was proposed in order to take into account implementation constraints. In this approach, the controlled signal has a special form:

$$u(t) = U(t)\cos\left(\phi_{exc}(t) + \phi_u(t)\right), \tag{3}$$

where $\phi_{exc}(t)$, named the excitation phase, is given and is assumed to be differentiable. The couple (U, ϕ_u) is referred to as a phasor of the signal u in the sequel. A complex phasor can be similarly defined: $\underline{u}(t) = U(t)e^{j\phi_u(t)}$.

In this approach, instead of computing $u(t)$, the controller computes $U(t)$ and $\phi_u(t)$ from the measurement of $Y(t)$ and $\phi_y(t)$ defined as:

$$y(t) = Y(t)\cos\left(\phi_{exc}(t) + \phi_y(t)\right), \tag{4}$$

that is the measure of the phasor of y. The control problem is then recast as the tracking and/or the rejection of phasor signals: compute the phasor $(U(t), \phi_u(t))$ such that the phasor $(Y(t), \phi_y(t))$ tracks a reference phasor $(Y_r(t), \phi_{y_r}(t))$.

In the usual case where y_r is a sinusoidal signal at frequency ω_0 and $\phi_{exc}(t) = \omega_0 t$, the reference signals $(Y_r(t), \phi_{y_r}(t))$ are actually constant. Since $u(t)$ and $y(t)$ are sinusoidal signals in steady state, $U(t)$, $\phi_u(t)$, $Y(t)$ and $\phi_y(t)$ are also constant.

As a consequence, in the phasor control problem, the to-be-controlled plant (input $(U(t), \phi_u(t))$, output $(Y(t), \phi_y(t)))$ is actually defined by (3), (2) and an operator which associates $(Y(t), \phi_y(t))$ to y, referred to in the sequel as s2p, that is:

$$\begin{cases} \dot{x}(t) = Ax(t) + BU(t)\cos\left(\phi_{exc}(t) + \phi_u(t)\right) \\ \begin{bmatrix} Y(t) \\ \phi_y(t) \end{bmatrix} = \mathrm{s2p}\left(Cx(t) + DU(t)\cos\left(\phi_{exc}(t) + \phi_u(t)\right)\right) \end{cases} \tag{5}$$

Since this operator and (3) are nonlinear, the design of the controller is a priori a difficult problem.

In the next section, we reveal that if the signals are replaced by their *complex* phasor, the (to-be-controlled) plant (5) becomes linear.

III. Complex phasor modeling

A. Complex phasor model

The following theorem introduces a (linear) model of the plant based on the complex phasors.

Theorem 1. *Given a differentiable function ϕ_{exc}, the ouput $y(t)$ of the system*

$$G: \begin{cases} \dot{x}(t) = Ax(t) + Bu(t) \\ y(t) = Cx(t) + Du(t) \end{cases}$$

for the input $u(t) = U(t)\cos\left(\phi_{exc}(t) + \phi_u(t)\right)$ is given by

$$y(t) = Y(t)\cos\left(\phi_{exc}(t) + \phi_y(t)\right),$$

where $(Y(t), \phi_y(t))$ is such that $Y(t) = |\underline{y}(t)|$, $\phi_y(t) = \arg(\underline{y}(t))$ and $\underline{y}(t)$ is the output of the system $\underline{G}$ defined by

$$\underline{G}: \begin{cases} \dot{\underline{x}}(t) &= \left(A - j\dot{\phi}_{exc}(t)I_n\right)\underline{x}(t) + B\underline{u}(t) \\ \underline{y}(t) &= C\underline{x}(t) + D\underline{u}(t) \end{cases} \tag{6}$$

for the input $\underline{u}(t) = U(t)e^{j\phi_u(t)}$.

Note that in (6), the signals $\underline{x}(t)$, $\underline{u}(t)$ and $\underline{y}(t)$ are actually complex. The system (6), which computes the complex phasor of y from the complex phasor of the input u, is linear parameter varying (LPV). Furthermore, in the important case when $\phi_{exc}(t) = \omega_0 t$, it is actually a linear time invariant system.

Proof. Let $\underline{y}(t)$ and $\underline{x}(t)$ be solutions of (6) for the input $\underline{u}(t) = U(t)e^{j\phi_u(t)}$. By multiplying (6) by $e^{j\phi_{exc}(t)}$, we have, after simplifications

$$\begin{cases} \frac{d}{dt}\left(\underline{x}(t)e^{j\phi_{exc}(t)}\right) &= A\underline{x}(t)e^{j\phi_{exc}(t)} + B\underline{u}(t)e^{j\phi_{exc}(t)} \\ \underline{y}(t)e^{j\phi_{exc}(t)} &= C\underline{x}(t)e^{j\phi_{exc}(t)} + D\underline{u}(t)e^{j\phi_{exc}(t)} \end{cases}.$$

By taking the real part, since A, B, C and D are real matrices, we obtain

$$\begin{cases} \frac{d}{dt}\left(\Re\left(\underline{x}(t)e^{j\phi_{exc}(t)}\right)\right) &= A\Re\left(\underline{x}(t)e^{j\phi_{exc}(t)}\right) + B\Re\left(\underline{u}(t)e^{j\phi_{exc}(t)}\right) \\ \Re\left(\underline{y}(t)e^{j\phi_{exc}(t)}\right) &= C\Re\left(\underline{x}(t)e^{j\phi_{exc}(t)}\right) + D\Re\left(\underline{u}(t)e^{j\phi_{exc}(t)}\right) \end{cases}$$

that corresponds to (2) with $u(t) = U(t)\cos\left(\phi_{exc}(t) + \phi_u(t)\right)$. □

The system $\underline{G}$, see (6), is referred to as the Complex Phasor Model (CPM) associated with G. The CPM is a system with complex-valued parameters. Nonetheless, by splitting the signals into real part and imaginary part, $\underline{G}$ can be equivalently represented by the following real-valued system, denoted complex phasor real model (CPRM):

$$G_{cp}: \left\{ \begin{array}{l} \dot{x}_{cp}(t) = A_{cp}\left(\dot{\phi}_{exc}(t)\right) x_{cp}(t) + B_{cp} u_{cp}(t) \\ y_{cp}(t) = C_{cp} x_{cp}(t) + D_{cp} u_{cp}(t) \end{array} \right. \tag{7}$$

with $x_{cp} = [\underline{x}_R^T \ \underline{x}_I^T]^T$, $u_{cp} = [\underline{u}_R^T \ \underline{u}_I^T]^T$, $y_{cp} = [\underline{y}_R^T \ \underline{y}_I^T]^T$,

$$A_{cp}\left(\dot{\phi}_{exc}(t)\right) = \begin{bmatrix} A & \dot{\phi}_{exc}(t) I_n \\ -\dot{\phi}_{exc}(t) I_n & A \end{bmatrix},$$

$B_{cp} = \mathrm{diag}(B, B)$, $C_{cp} = \mathrm{diag}(C, C)$ and $D_{cp} = \mathrm{diag}(D, D)$. Note that this model corresponds to the system

$$\left\{ \begin{array}{l} \dot{x}(t) = Ax(t) + B\left[\cos\left(\phi_{exc}(t)\right) - \sin\left(\phi_{exc}(t)\right)\right] u_{cp}(t) \\ y_{cp}(t) = \mathrm{s2cp}\left(Cx(t) + D\left[\cos\left(\phi_{exc}(t)\right) - \sin\left(\phi_{exc}(t)\right)\right] u_{cp}(t)\right) \end{array} \right.$$

where x is the state space vector of (5) and s2cp is an operator which associates y_{cp} to y.

Based on the model (7), we can define a new control problem, denoted **complex phasor control problem**. For the sake of simplicity, we focus on the case when $\phi_{exc}(t) = \omega_0 t$, that is, G_{cp} is an LTI system. The general case can be similarly discussed using the LPV control approach, see *e.g.* [5].

In this problem, the plant is defined by $\underline{G}$, see (6) (resp. G_{cp}, see (7)), and the controller denoted $\underline{K}$ (resp. K_{cp}), has to compute $\underline{u}$ (resp. u_{cp}) from the measurement of $\underline{y}$ (resp. y_{cp}), such that $\underline{y}$ tracks the reference signal $\underline{y}_r$ (resp. $y_{r_{cp}}$).

Before to proceed with the control design, we present some relevant properties of the complex phasor model in the LTI case.

B. Properties of the complex phasor model in the LTI case

Since $\underline{G}$ and G_{cp} have poles with the same real part that the poles of G, the stability of one is equivalent to the stability of the other ones [6]. Since $\underline{G}$ can be defined as [7], [8]

$$\underline{G}(s) = G(s + j\omega_0),$$

the frequency response of $\underline{G}$ corresponds to a frequency shift of the frequency response of G. Moreover, the H_∞-norm of G is equal to the H_∞-norm of $\underline{G}$ which is equal to the H_∞-norm of G_{cp}, see [8].

IV. Control design based on the direct problem

In this section, we intend to answer two key questions:

(i) Considering the direct control and the complex phasor control approaches, does any of them ensure a better performance level?

(ii) Is it possible to compute a direct control law and transform it into a complex phasor control law, since a strong motivation for considering this approach is to respect implementation constraints?

We first define the performance level as an upper bound on the H_∞-norm of the interconnection of the augmented plant, that is, the plant augmented with weighting functions and the controller [4]. Note that the discussion holds true for other performance criteria, based on, *e.g.*, the H_2 norm.

A. Solving the direct control problem and the complex phasor control problem

The control law for the direct control problem can be computed by solving the standard H_∞ problem. We consider an augmented plant P, composed by the plant G and weighting functions (for further details, see [4]), usually defined by a state-space representation

$$P: \left\{ \begin{array}{lclclcl} \dot{x}_P(t) & = & A_P x_P(t) & + & B_u u_P(t) & + & B_w w(t) \\ y_P(t) & = & C_y x_P(t) & & & + & D_{yw} w(t) \\ z(t) & = & C_z x_P(t) & + & D_{zu} u_P(t) & + & D_{zw} w(t) \end{array} \right. \tag{8}$$

The problem is: given $\gamma > 0$, compute a controller

$$K: \left\{ \begin{array}{rcl} \dot{x}_K(t) & = & A_K x_K(t) + B_K y_P(t) \\ u_P(t) & = & C_K x_K(t) + D_K y_P(t) \end{array} \right. , \tag{9}$$

if there is any, such that $\|P \star K\|_\infty < \gamma$, where $P \star K$ denotes the Redheffer product of P and K, that is, the closed loop system defined by (8) and (9).

The following theorem allows testing if this problem has a solution.

Theorem 2 ([9])**.** *Consider the system* (8)*. There is a dynamic output feedback, in the form of* (9)*, such that* $\|P \star K\|_\infty < \gamma$ *if and only if there exist* $R, S \in \mathbb{R}^{n \times n}$ *such that* $R = R^T$, $S = S^T$,

$$\left[\diamond\right]_\perp^T \begin{bmatrix} SA_P^T + A_P S & B_w & SC_z^T \\ B_w^T & -\gamma I & D_{zw}^T \\ C_z S & D_{zw} & -\gamma I \end{bmatrix} \begin{bmatrix} B_u^T & 0 & D_{zu}^T \end{bmatrix}_\perp \prec 0,$$

$$\left[\diamond\right]_\perp^T \begin{bmatrix} A_P^T R + R A_P & R B_w & C_z^T \\ B_w^T R & -\gamma I & D_{zw}^T \\ C_z & D_{zw} & -\gamma I \end{bmatrix} \begin{bmatrix} C_y & D_{yw} & 0 \end{bmatrix}_\perp \prec 0$$

$$\textit{and} \quad \begin{bmatrix} R & I \\ I & S \end{bmatrix} \succ 0.$$

The complex phasor control problem can be addressed as a special case of the H_∞ control problem, with a new augmented plant P_{cp} which is the complex phasor real model associated to the augmented plant P. Nevertheless, the solution $\underset{\sim}{K}$ of this H_∞ control problem does not necessarily admit a state space representation which has the structure of a complex phasor real model.

Since the direct control problem and the complex phasor one can be formulated as an H_∞ control problem, in the next subsection we consider this formalism to investigate the links between them.

B. Connections between the direct control problem and the complex phasor real control problem

We now investigate the connections between the direct control problem and the complex phasor one.

Theorem 3. *Let P be the augmented plant defined by* (8) *and K the controller defined by* (9)*. Let P_{cp} and K_{cp} be respectively the CPRM of P and K for $\phi_{exc}(t) = \omega_0 t$. Then, given $\gamma > 0$,*

1) *if K is such that $\|P \star K\|_\infty < \gamma$ then $\|P_{cp} \star K_{cp}\|_\infty < \gamma$;*
2) *$\|P \star K\|_\infty = \|P_{cp} \star K_{cp}\|_\infty$;*
3) *there exists a controller $\underset{\sim}{K}$ such that $\|P_{cp} \star \underset{\sim}{K}\|_\infty < \gamma$ if and only if there exists K such that $\|P \star K\|_\infty < \gamma$.*

The first property presented in the theorem claims that if a direct control law K achieves a given performance level γ, then the phasor model K_{cp} of K is a solution of the complex phasor control problem, ensuring the same performance level. Furthermore, according to the second property, the H_∞-norm of the closed-loop systems are equal.

The third property reveals that if the H_∞ solution $\underset{\sim}{K}$ of the complex phasor control problem achieves a given performance level then, necessarily, the same level of performance can be obtained by a direct control law and vice-versa. In other words, even with an augmented degree of freedom (number of variables), the complex phasor control problem cannot ensure a better performance level than that of the direct control.

Proof. Properties 1) & 2): they can be proved by building the state-space realisations of $(P \star K)_{cp}$ and $P_{cp} \star K_{cp}$ from the state-space realisations of P and K and by observing that both realisations are the same, *i.e.*, $P_{cp} \star K_{cp} = (P \star K)_{cp}$. For the sake of briefness, the details based on routine algebra are omitted. As $\|(P \star K)_{cp}\|_\infty = \|P \star K\|_\infty$, then $\|P \star K\|_\infty = \|P_{cp} \star K_{cp}\|_\infty$, which proves property 1 and property 2.

Property 3): here, we just present the sketch of the proof. Details are developed in Appendix A. The proof consists in first applying the H_∞ problem associated to the direct control problem. The existence of K such that $\|P \star K\|_\infty < \gamma$ is equivalent to the fact that the feasibility problem defined by Theorem 2 has a solution. The second step consists in using the solution of this feasibility problem to construct the solution of the feasibility problem defined by Theorem 2 when this theorem is applied to the complex phasor control problem, which

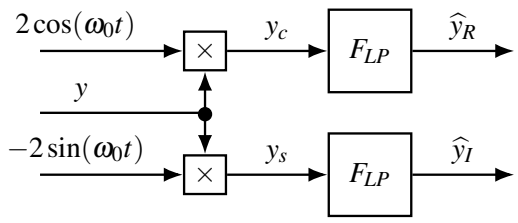

Fig. 2. Block-diagram of the synchronous demodulation.

implies that there exists $\underset{\sim}{K}$ such that $\|P_{cp} \star \underset{\sim}{K}\|_\infty < \gamma$. The same procedure is applied in the other sense, changing the direct problem by the complex phasor problem and vice-versa. □

All these results are based on the fact that (5) is exactly described by G_{cp}. Nonetheless, we will discuss in the next section that the ideal s2cp block cannot be implemented in practice. To extract amplitude and phase of a signal (or equivalently the real and imaginary parts), nonlinear operators and filters are introduced into the loop. These additional elements, that were not taken into consideration in this section, may drastically degrade the performance of the closed-loop system or even make it unstable. Thus, in the next section, we present how to implement the s2cp block and how to model its nonidealities. Then, we propose an approach to take into account these nonidealities during the control design.

V. Implementation of s2cp and robust control design

Up to this point, we have considered the s2cp block as an operator that allows to extract y_{cp} from a signal y. Nonetheless, by observing (4), one can notice that, for a given ϕ_{exc} and y, an infinity number of couples (Y, ϕ_y), and consequently $(\underline{y}_R, \underline{y}_I)$, satisfies the equation. This ambiguity problem is recurrent in communication theory and signal processing (see *e.g.* [10], [11]) and can be solved by means of the Hilbert transform. In practice, this operation is performed by a synchronous demodulation, that will introduce some nonidealities into the s2cp block. Therefore, in this section, we aim to discuss the implementation of the s2cp block and how to model its nonidealities. Then, we propose a control design method that takes into account these nonidealities.

A. Implementation of the s2cp block

In practice (and for $\phi_{exc}(t) = \omega_0 t$), the operator s2cp can be implemented by a synchronous demodulation if the power spectrum of y is in the interval $(0,\, 2\omega_0)$ [10]. Fig. 2 presents the structure of the demodulator, which includes **ideal** low-pass filters F_{LP} with cutoff frequency $\omega_c = \omega_0$. This structure is motivated by the following point. Let $\underline{y}$ be the complex phasor of y, *i.e.*, $y(t) = \underline{y}_R(t)\cos(\omega_0 t) - \underline{y}_I(t)\sin(\omega_0 t)$. Thus, the signals $y_c(t) = 2y(t)\cos(\omega_0 t)$ and $y_s(t) = -2y(t)\sin(\omega_0 t)$ can be rewritten as

$$\begin{aligned} y_c(t) &= \underline{y}_R(t) + \overbrace{\Big(\underline{y}_R(t)\cos(2\omega_0 t) - \underline{y}_I(t)\sin(2\omega_0 t)\Big)}^{\delta \underline{y}_R(t)} \\ y_s(t) &= \underline{y}_I(t) - \underbrace{\Big(\underline{y}_R(t)\sin(2\omega_0 t) + \underline{y}_I(t)\cos(2\omega_0 t)\Big)}_{\delta \underline{y}_I(t)}. \end{aligned} \tag{10}$$

As the power spectrum support of the signal y is assumed to be included in the frequency interval $(0, 2\omega_0)$, then the power spectrum support of $\underline{y}_R(t)$ and $\underline{y}_I(t)$ is in $(0,\, \omega_0)$, and the power spectrum support of $\delta\underline{y}_R(t)$ and $\delta\underline{y}_I(t)$ is in $(\omega_0,\, 3\omega_0)$. As a consequence, since F_{LP} is an ideal filter with $\omega_c = \omega_0$, then $\widehat{y}_R(t) = \underline{y}_R(t)$ and $\widehat{y}_I(t) = \underline{y}_I(t)$.

In practice however, the low-pass filter is not ideal. Indeed, it presents a transition band between the pass band and the stop band. Since the power spectrum support of $\delta\underline{y}_R(t)$ and the power spectrum support of $\underline{y}_R(t)$ can be very close, the existence of the transition band can dramatically change the behavior of the closed-loop system. Therefore, it is crucial to:

1) evaluate the effect of this nonideal filter when the control law was computed as described in section IV, with the assumption that the s2cp block was ideal; this *a posteriori* analysis is investigated in [12];
2) to take this nonideality into account for the computation of the control law. This point is developed in the next section.

B. Complex phasor control with nonideal s2cp

Now, the question is how to model the nonideal s2cp, *i.e.*, the synchronous demodulation with nonideal F_{LP}. From (10), y_c and y_s can be rewritten in matrix form as

$$\begin{bmatrix} y_c(t) \\ y_s(t) \end{bmatrix} = (I+\Delta(\omega_0)) \begin{bmatrix} \underline{y}_R(t) \\ \underline{y}_I(t) \end{bmatrix}$$

with

$$\Delta(\omega_0) = \begin{bmatrix} \cos(2\omega_0 t) & -\sin(2\omega_0 t) \\ -\sin(2\omega_0 t) & -\cos(2\omega_0 t) \end{bmatrix}.$$

Hence, the nonideal s2cp (synchronous demodulation) may be modeled as the series connection of an ideal s2cp, the block $(I+\Delta(\omega_0))$ and the nonideal filters F_{LP}, as illustrated in Fig. 3. The strong interest of this modeling is that the to-be-controlled system is represented as a serial connection of the CPRM and associated nonidealities of the s2cp block.

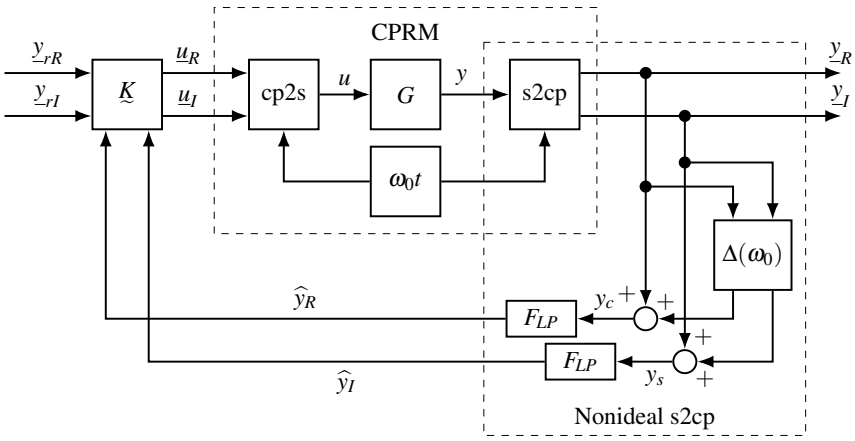

Fig. 3. Block-diagram of the complex phasor architecture with nonideal s2cp

In the sequel, this modeling is used to propose a method for computing the CPRM controller $\underset{\sim}{K}$ by explicitly taking into account the nonideal s2cp.

C. Solution to the complex phasor control problem with nonideal s2cp

In this section, we propose a solution of the complex phasor control problem which takes into account the two elements of the nonideal s2cp: the nonideal filtering and the time-varying matrix $\Delta(\omega_0)$. The closed-loop system has to satisfy some performance specifications: stability, constant reference tracking with a maximum allowed steady-state error and constant disturbance rejection. To this purpose, we consider the control architecture presented in Fig. 4, where $y_{r_{cp}}$ is the reference, ε_{cp} the tracking error, d_{cp} the input disturbance and n_{cp} represents the disturbance provoked by the time-varying matrix $\Delta(\omega_0)$.

In the H_∞ synthesis approach, the solution is obtained by finding $\underset{\sim}{K}$, if there is any, such that the following H_∞ criterion is ensured:

$$\left\| \begin{matrix} \mathrm{diag}(W_\varepsilon, W_\varepsilon) T_{y_{r_{cp}} \to \varepsilon_{cp}} \mathrm{diag}(W_r, W_r) & \mathrm{diag}(W_\varepsilon, W_\varepsilon) T_{d_{cp} \to \varepsilon_{cp}} \mathrm{diag}(W_d, W_d) & \mathrm{diag}(W_\varepsilon, W_\varepsilon) T_{n_{cp} \to \varepsilon_{cp}} \mathrm{diag}(W_n, W_n) \\ \mathrm{diag}(W_u, W_u) T_{y_{r_{cp}} \to u_{cp}} \mathrm{diag}(W_r, W_r) & \mathrm{diag}(W_u, W_u) T_{d_{cp} \to u_{cp}} \mathrm{diag}(W_d, W_d) & \mathrm{diag}(W_u, W_u) T_{n_{cp} \to u_{cp}} \mathrm{diag}(W_n, W_n) \end{matrix} \right\|_\infty < 1, \tag{11}$$

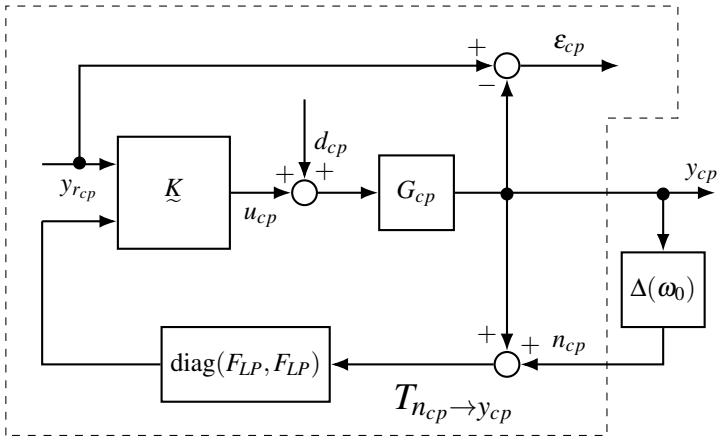

Fig. 4. Control architecture considered for the complex phasor control with nonideal s2cp.

where $T_{a\to b}$ denotes the transfer from signal a to signal b and

$$W_\varepsilon(s) = \frac{\frac{1}{M_\varepsilon}s + \omega_\varepsilon^*}{s + \omega_\varepsilon^* A_\varepsilon}, \quad W_u(s) = \frac{s + \omega_u^* A_u}{\frac{1}{M_u}s + \omega_u^*},$$

$$W_r(s) = k_r, \quad W_d(s) = k_d, \quad W_n(s) = W_\varepsilon(s)^{-1}$$

with the user chosen parameters $A_\varepsilon \leq 1$, $M_\varepsilon \geq 1$, ω_ε^*, $A_u \leq 1$, $M_u \geq 1$, ω_u^*, k_r and k_d, detailed in the sequel. This H_∞ criterion is represented in Fig. 5, where the weighting functions W_x express the control specifications [4], as detailed thereafter.

- *Reference tracking:* (11) implies that

$$\forall\omega, \quad |T_{y_{r_R}\to\varepsilon_R}(j\omega)| \leq \frac{1}{|W_\varepsilon(j\omega)W_r(j\omega)|} \quad \text{and} \quad \forall\omega, \quad |T_{y_{r_I}\to\varepsilon_I}(j\omega)| \leq \frac{1}{|W_\varepsilon(j\omega)W_r(j\omega)|} \ ,$$

  which ensures the tracking of constant y_{r_R} and y_{r_I} by y_R and y_I with a static error bounded by $A_\varepsilon k_r$ and the convergence speed is constrained by ω_ε^*, that is, it enforces a lower bound on the time response. For further details, see *e.g.* [4].
- *Disturbance rejection:* (11) implies that

$$\forall\omega, \quad |T_{d_R\to\varepsilon_R}(j\omega)| \leq \frac{1}{|W_\varepsilon(j\omega)W_d(j\omega)|} \quad \text{and} \quad \forall\omega, \quad |T_{d_I\to\varepsilon_I}(j\omega)| \leq \frac{1}{|W_\varepsilon(j\omega)W_d(j\omega)|},$$

  which ensures disturbance rejection of constant d_R and d_I with a static error bounded by $A_\varepsilon k_d$ and a bandwidth constraints by ω_ε^*.
- *Control limitation:* (11) implies that

$$\begin{aligned} &\forall\omega, \quad |T_{y_{r_R}\to u_R}(j\omega)| \leq \frac{1}{|W_u(j\omega)W_r(j\omega)|} \quad \text{and} \quad \forall\omega, \quad |T_{y_{r_I}\to u_I}(j\omega)| \leq \frac{1}{|W_u(j\omega)W_r(j\omega)|} \\ &\forall\omega, \quad |T_{d_R\to u_R}(j\omega)| \leq \frac{1}{|W_u(j\omega)W_d(j\omega)|} \quad \text{and} \quad \forall\omega, \quad |T_{d_I\to u_I}(j\omega)| \leq \frac{1}{|W_u(j\omega)W_d(j\omega)|}, \end{aligned}$$

  which constraints by ω_u^* the bandwidth of the two-degree-of-freedom controller.
- *Nonideal s2cp:* (11) implies that :

$$\|\,\mathrm{diag}(W_\varepsilon, W_\varepsilon)T_{n_{cp}\to\varepsilon_{cp}}\,\mathrm{diag}(W_n, W_n)\|_\infty < 1.$$

  Since $W_n = W_\varepsilon{}^{-1}$ and $T_{n_{cp}\to\varepsilon_{cp}} = -T_{n_{cp}\to y_{cp}}$, we have that the previous inequality implies $\|T_{n_{cp}\to y_{cp}}\|_\infty < 1$. As the L_2 gain of an LTI system is equal to its H_∞ norm [13], the L_2 gain of $T_{n_{cp}\to y_{cp}}$ is strictly less than 1. Note that the nonideal closed-loop system presented in Fig. 4 can be rewritten as the interconnection of $T_{n_{cp}\to y_{cp}}$ and $\Delta(\omega_0)$. Since

$$\forall\, t, \omega_0 \in \mathbb{R}, \quad \overline{\sigma}(\Delta(\omega_0)) \leq 1$$

  the L_2 gain of the operator which to y_{cp} associates $\Delta(\omega_0)y_{cp}$ is less or equal to 1. Then, since the product of the L_2 gain of this operator and the L_2 gain of $T_{n_{cp}\to y_{cp}}$ is strictly less than 1, the stability of overall interconnected system is obtained by applying the small gain theorem [13].

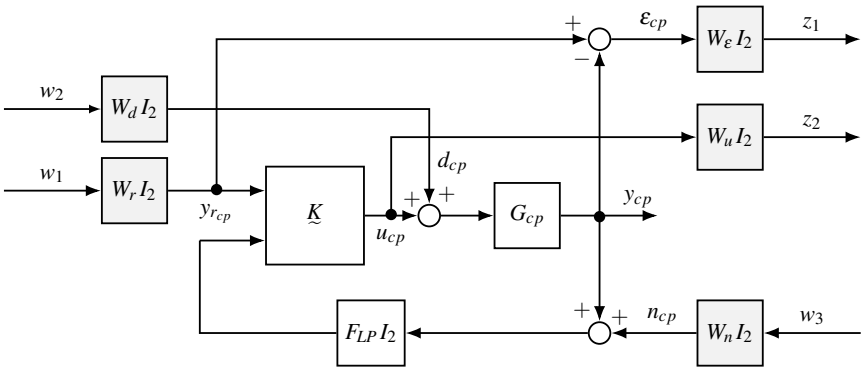

Fig. 5. Considered criterion for the H_∞ synthesis.

VI. Numerical examples

In this section, we illustrate the different control approaches considered in this paper. We consider three different cases. For the first two ones, we design a controller in the direct approach. Then, we take its corresponding CPRM to apply in a phasor approach, as presented in section IV. The third case consists of the synthesis taking the s2p nonidealities into account, as discussed in section V.

For this example, we consider the control of a MEMS gyroscope. This type of device is composed of two perpendicular resonant modes: the primary mode and the secondary one. Oscillations are driven on the primary mode. Then, if the gyroscope is submitted to an angular rate perpendicular to those axes, oscillations are provoked on the secondary mode due to the Coriolis effect. Hence, by measuring these secondary oscillations, the angular rate is estimated. To ensure high accuracy of the measurements, control loops are used, see *e.g.*, [1], [2]. Here, we focus on the control of the primary mode, that shall drive oscillations with a controlled amplitude. Moreover, to avoid saturation of the control signal, the oscillations shall be driven around the resonance frequency of the primary mode. This system can be modeled by (2) with

$$A = \begin{bmatrix} 0 & 1 \\ -\omega_n^2 & -\omega_n/Q \end{bmatrix}, \quad B = \begin{bmatrix} 0 \\ \omega_n \end{bmatrix}, \quad C = \begin{bmatrix} 1 & 0 \end{bmatrix}, \quad D = 0,$$

with the natural frequency $\omega_n = 2\pi \cdot 11500\ \mathrm{rad\,s^{-1}}$ and the quality-factor $Q = 50$.

Then, for this application, we consider the following specifications:

1) the tracking of a reference signal in the form $y_r(t) = Y_r \cos(\omega_0 t)$ with $\omega_0 = \omega_n$ and an error $\varepsilon(t) = y_r(t) - y(t)$ is ensured, such that $|\varepsilon(t)| < 0.002 Y_r$ in steady-state (*i.e.* $0,2\%$ of the reference amplitude); moreover, the steady-state is achieved in less than $0.5\,\mathrm{ms}$;
2) the amplitude of the control signal is less than 0.5 units;
3) the closed-loop system is stable, *i.e.* the stability against the nonidealities of the s2cp has to be guaranteed.

A. Study case 1: design based on the direct control problem (two degrees of freedom)

In this first case, we consider a two-degrees-of-freedom controller that has two inputs: the reference signal y_r as well as the system output y. This controller computes the control signal u which is applied to G. Thus, we consider an H_∞ synthesis with the criterion presented in Fig. 6 in order to compute K, if there is any, such that:

$$\left\| \begin{matrix} W_\varepsilon T_{y_r \to \varepsilon} W_r & W_\varepsilon T_{d \to \varepsilon} W_d & W_\varepsilon T_{n \to \varepsilon} W_n \\ W_u T_{y_r \to u} W_r & W_u T_{d \to u} W_d & W_u T_{n \to u} W_n \end{matrix} \right\|_\infty < 1. \tag{12}$$

This H_∞ criterion is similar to the one presented in (11) and Fig. 5, except that the nonidealities of the synchronous demodulation are not explicitly taken into account, the signals of the closed-loop system are scalars and the weighting function used are modified. Indeed, as mentioned before, in contrast to the complex phasor control problem, in the direct control problem, the reference and disturbance signals are sinusoidal and not constant signals. The weighting filters are thus given by

$$W_\varepsilon(s) = \frac{1}{M_\varepsilon} \frac{s^2 + \alpha_\varepsilon s + \omega_0^2}{s^2 + \alpha_\varepsilon A_\varepsilon / M_\varepsilon \cdot s + \omega_0^2}, \quad W_u(s) = M_u \frac{s^2 + \alpha_u A_u / M_u \cdot s + \omega_0^2}{s^2 + \alpha_u s + \omega_0^2},$$

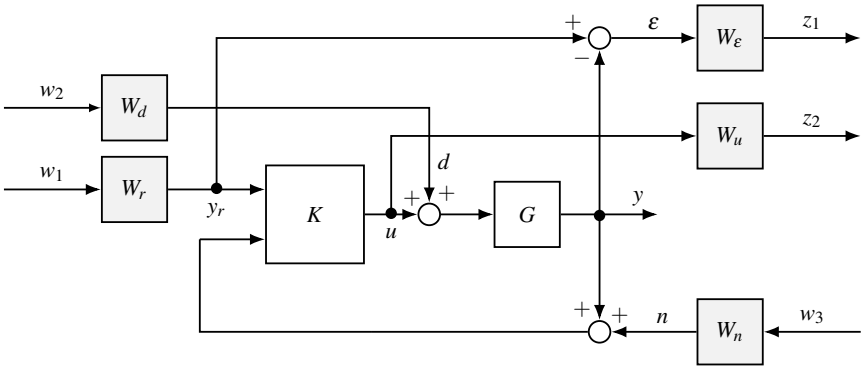

Fig. 6. Criterion for the H_∞ synthesis for the study case 1.

$$W_r(s) = k_r, \quad W_d(s) = k_d, \quad W_n(s) = k_n,$$

where the choice of the parameters $A_\varepsilon \leq 1$, $M_\varepsilon \geq 1$, α_ε, $A_u \leq 1$, $M_u \geq 1$, α_u, k_r and k_d is detailed in the sequel. These weighting functions express the following control specifications [4]:

- *reference tracking:* (12) implies that

$$\forall \omega, \quad |T_{y_r \to \varepsilon}(j\omega)| \leq \frac{1}{|W_\varepsilon(j\omega) W_r(j\omega)|} \ ,$$

  which ensures the tracking of sinusoidal reference signal y_r by y with a frequency ω_0 and error bounded by $A_\varepsilon k_r$ and convergence speed constrained by α_ε;
- *control limitation:* (12) implies that

$$\forall \omega, \quad |T_{y_r \to u}(j\omega)| \leq \frac{1}{|W_u(j\omega) W_r(j\omega)|} \quad \text{and} \quad \forall \omega, \quad |T_{d \to u}(j\omega)| \leq \frac{1}{|W_u(j\omega) W_d(j\omega)|},$$

  which constrains by α_u the bandwidth of the controller and by A_u, M_u the control signal power and therefore its amplitude [4];
- *robustness against the s2cp nonidealities:* since we consider the direct control problem, this specification is not taken into consideration for the controller design. In the present case, the robustness with respect to the nonidealities of the s2cp is evaluated in simulation.

To respect these specifications, we choose the parameters presented in Table I.

TABLE I

PARAMETERS FOR THE CONTROLLER DESIGN OF THE STUDY CASE 1

Parameter	Value	Parameter	Value
A_ε	$1.25 \cdot 10^{-3}$	A_u	$2.5 \cdot 10^{-2}$
M_ε	2	M_u	$2.5 \cdot 10^{3}$
α_ε	$0.5538\omega_0$	α_u	$1056\omega_0$
k_r	1	k_d	$1 \cdot 10^{-3}$
k_n	0.5		

By solving the H_∞ problem we find the controller $K = [K_r \ K_y]$, ensuring (12) with:

$$K_r(s) = 2.59 \cdot 10^{-4} \frac{(s+1382\omega_n)(s-0.8647\omega_n)(s+5.852 \cdot 10^{-4}\omega_n)(s^2+0.0206\omega_n s+\omega_n^2)}{(s+0.5309\omega_n)(s^2+3.9 \cdot 10^{-4}\omega_n s+\omega_n^2)(s^2+1.353\omega_n s+1.629\omega_n^2)}$$

$$K_y(s) = -5.65 \cdot 10^{-5} \frac{(s+6359\omega_n)(s-0.865\omega_n)(s+4.441 \cdot 10^{-4}\omega_n)(s^2+0.0205\omega_n s+\omega_n^2)}{(s+0.5309\omega_n)(s^2+3.9 \cdot 10^{-4}\omega_n s+\omega_n^2)(s^2+1.353\omega_n s+1.629\omega_n^2)}$$

This controller is then transformed into a phasor controller K_{cp} via Theorem 1 and implemented according to the phasor-based architecture.

To evaluate the tracking performance of the obtained controller, we apply an amplitude reference step at $t = 1$ ms and $\omega_0 = \omega_n$, as shown in Fig. 7. The closed loop composed of K and G is referred to as direct approach, whereas the control loop composed by K_{cp} and G_{cp} is denoted ideal CPRM.

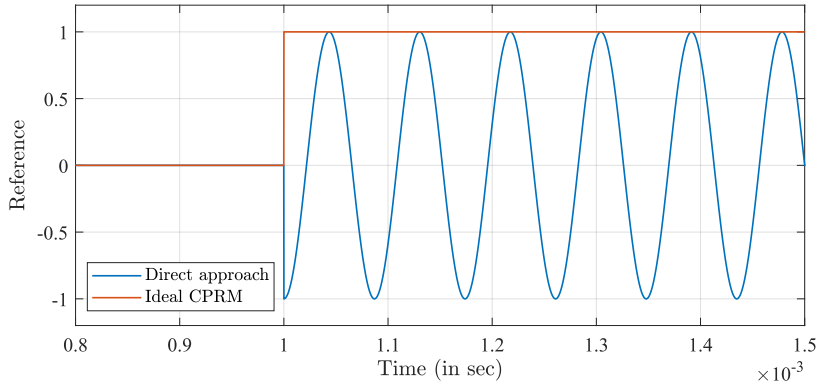

Fig. 7. Study case 1 - reference signal.

TABLE II

PARAMETERS FOR THE CONTROLLER DESIGN OF THE STUDY CASE 2

Parameter	Value	Parameter	Value
A_ε	$1.25 \cdot 10^{-3}$	A_u	$5 \cdot 10^{-6}$
M_ε	2	M_u	$5 \cdot 10^{3}$
ω_ε^* (in $\mathrm{rad\,s^{-1}}$)	$1.154 \cdot 10^{4}$	ω_u^* (in $\mathrm{rad\,s^{-1}}$)	$1.669 \cdot 10^{4}$
k_r	1	k_d	$1 \cdot 10^{-3}$

The output, tracking error and the control signal of both strategies are presented in Fig. 8. We observe that, in about 0.3 ms, the error of the direct approach converges to its steady-state value, that is close to 0.11% of Y_r. For the sake of illustration, we present only the amplitude computed from the ideal CPRM, that corresponds to the amplitude envelope of the error of the direct approach. If we reconstruct a signal from the amplitude and phase shift (or equivalently from real and imaginary parts), we obtain exactly the same signal produced in the direct approach. This fact illustrates the Theorem 1 and validates the discussions of section IV.

In order to evaluate the behavior of the closed-loop system with the nonideal s2cp, we simulate the overall system with

$$F_{LP}(s) = \frac{\omega_c}{s + \omega_c}$$

and $\omega_c = 2\pi \cdot 100\,\mathrm{rad\,s^{-1}}$. The simulation results are presented in Fig. 9, where we notice that the error has higher values and takes more than 20 ms to achieve steady-state. When in steady-state, the amplitude error is about 0.46% of Y_r. These substantial differences with respect to the ideal CPRM are due to the nonideal filter. During the transient state, the filter slows down the output measure. Then, the controller applies stronger actions, what is actually not necessary, justifying the important amplitude overshoot. When, the system achieves the steady-state, the harmonics generated by the synchronous demodulation are not completely eliminated by the filter, then these components disturb the system and produce an error that is bigger than the one in the ideal case.

Besides the important changes on the behavior of the closed-loop system, if we reduce the cutoff frequency of the nonideal filter, the system may become unstable. To illustrate this fact, we make $\omega_c = 2\pi \cdot 8\,\mathrm{rad\,s^{-1}}$. The simulation results are presented in Fig. 10, where the tracking error diverges.

B. Study case 2: design based on the CPRM and nonideal s2cp

In this case, we illustrate the method presented in section V, where the nonidealities of the synchronous demodulation are taken into account for the design of the controller. Furthermore, we consider F_{LP} with $\omega_c = 2\pi 8\,\mathrm{rad\,s^{-1}}$, which makes the closed-loop system of the previous study case unstable.

To respect the requirement specifications, we consider the criterion and weighting functions presented in section V-C with the parameters presented in Table II.

Then, with the H_∞ synthesis, we obtain a controller that ensures, in addition to the reference tracking and control limitation performance (at a similar level than in the ideal case example), $\|T_{n_{cp} \to y_{cp}}\|_\infty = 0.983$. Hence,

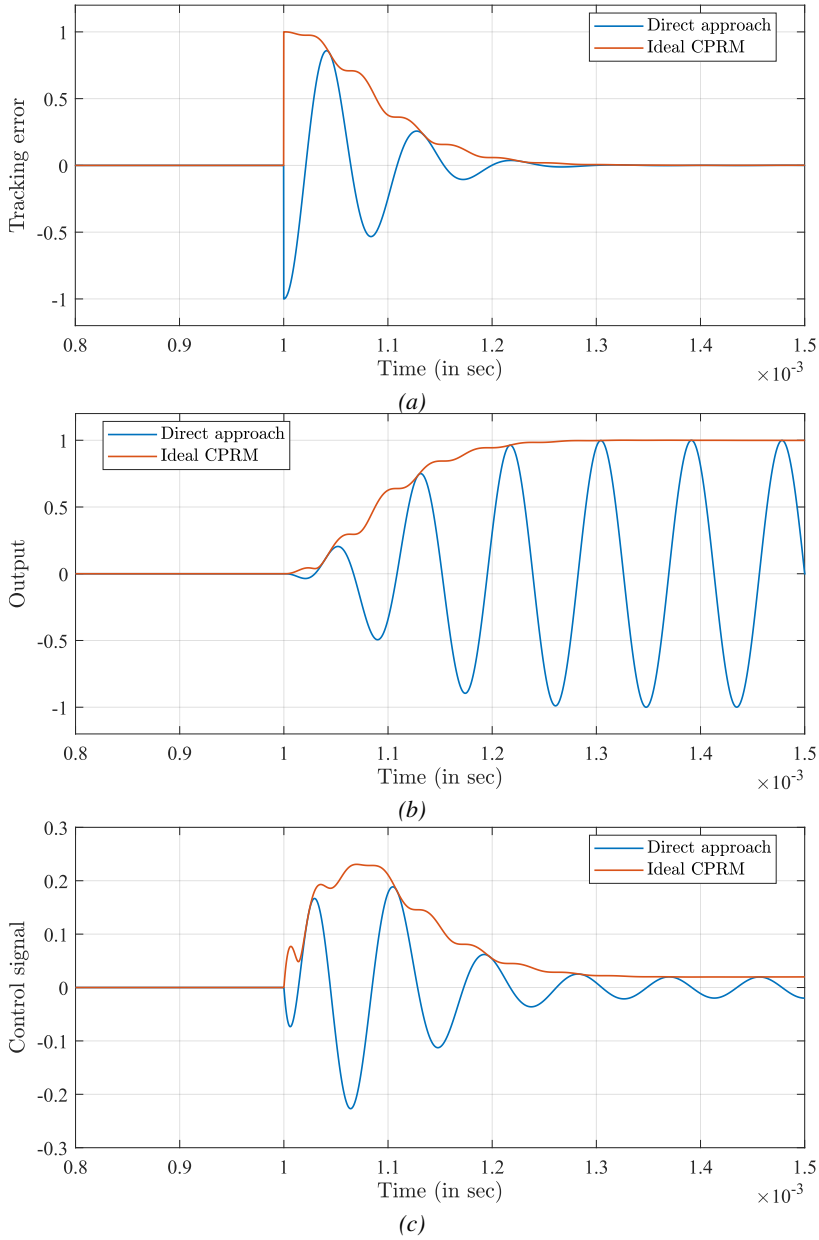

Fig. 8. Study case 1 - comparison between direct approach (G, K) and ideal CPRM (G_{cp}, K_{cp}) for a two-degree-of-freedom controller.

the small gain theorem conditions are satisfied and ensure the stability of the closed-loop system in presence of the time-varying matrix $\Delta(\omega_0)$.

This controller is applied according to a phasor-based architecture with a nonideal s2cp and F_{LP} with $\omega_c = 2\pi \cdot 8\,\mathrm{rad\,s^{-1}}$. We apply the same reference signal of the previous study case, see Fig. 7. For the sake of comparison, we also consider the results of the direct approach presented previously. The tracking errors, as well as the outputs and control signals, are presented in Fig. 11, where we can notice that, despite the nonideal s2cp, at the transient-state, both strategies present a very similar behavior. The phasor approach presents some small oscillations until $t \approx 3\,\mathrm{ms}$. In steady-state, the tracking errors of both strategies converge to close to 0.1% of Y_r, as specified at the beginning of the section.

C. Study case 3: design based on the direct problem (one degree of freedom)

In this last case, we simulate a simplified version of the study case 1. Here, a direct approach with a one-degree-of-freedom controller is considered. This controller is by with the H_∞ approach with the criterion presented in

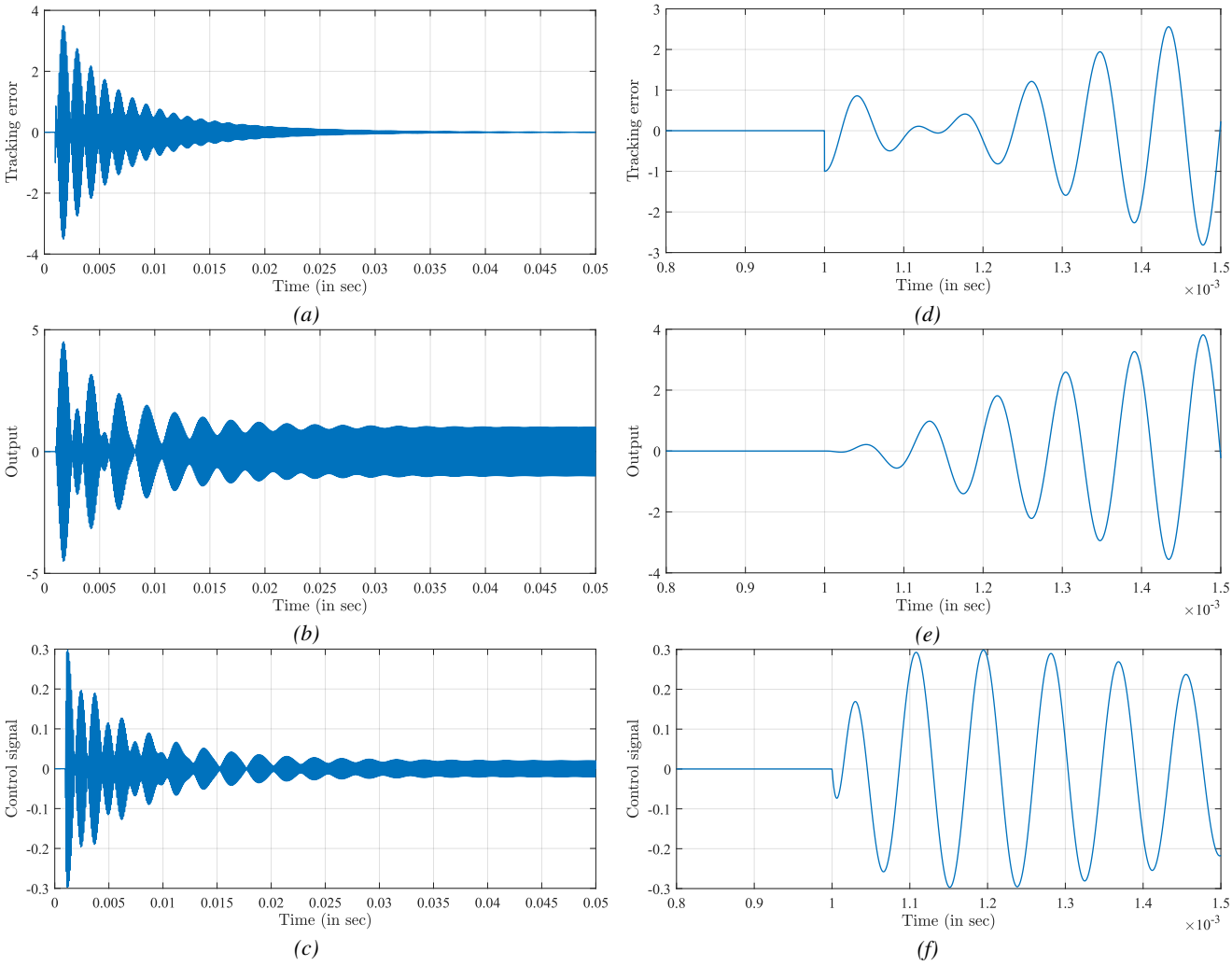

Fig. 9. Study case 1 - CPRM (G_{cp}, K_{cp}) with nonideal s2cp and $\omega_c = 2\pi \cdot 100\,\mathrm{rad\,s^{-1}}$. *(a)* tracking error, *(b)* output and *(c)* control signal in a long time scale; zoom of *(d)* tracking error, *(e)* output and *(f)* control signal.

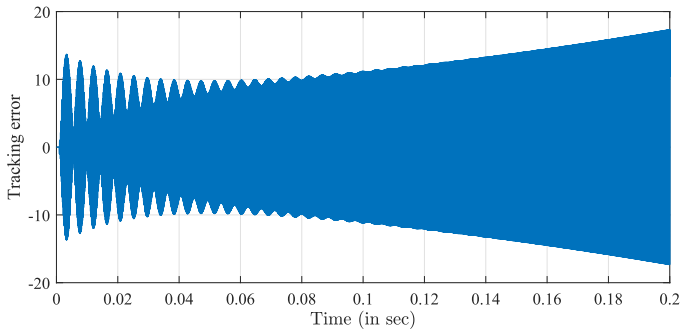

Fig. 10. Study case 1 - CPRM (G_{cp}, K_{cp}) with nonideal s2cp and $\omega_c = 2\pi \cdot 8\,\mathrm{rad\,s^{-1}}$.

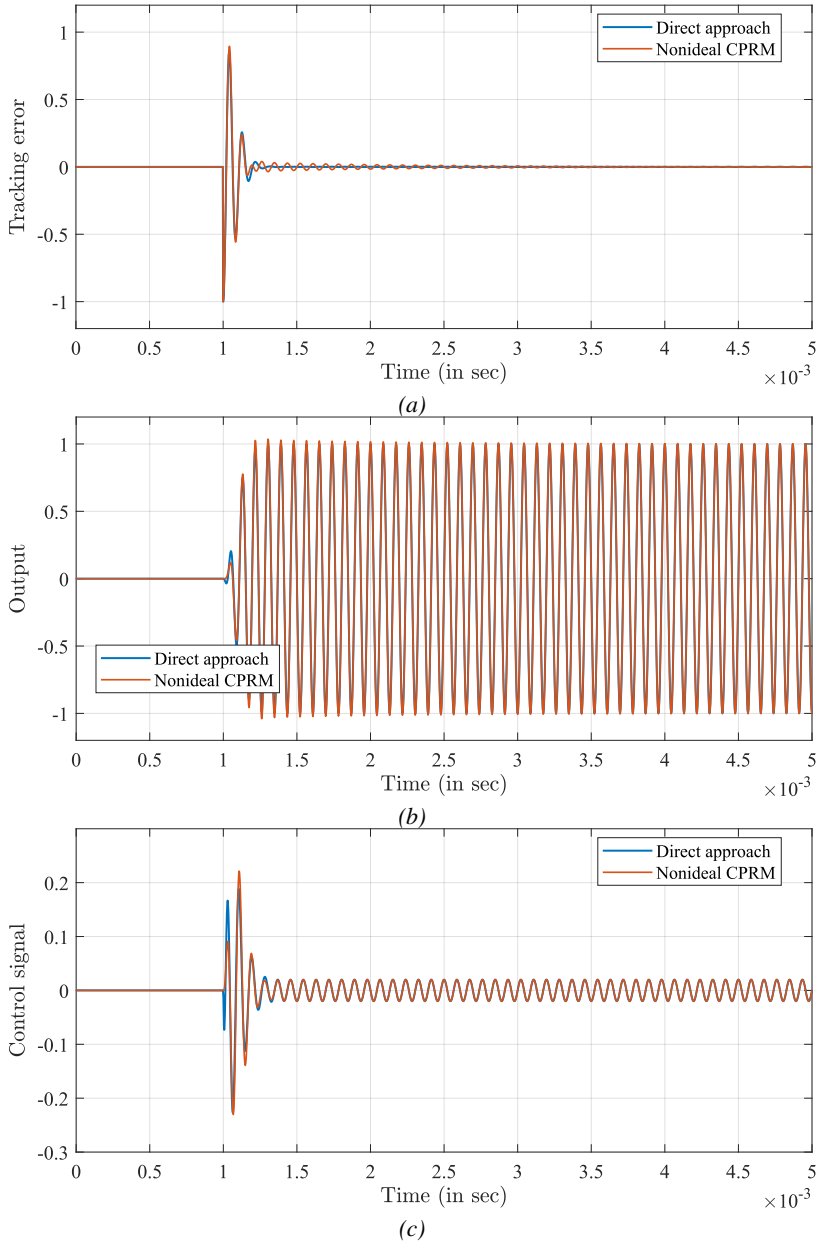

Fig. 11. Study case 2 - comparison between direct approach (G, K) and nonideal CPRM $(G_{cp}, \tilde{K})$.

Fig. 12, known as 4-block criterion [4], *i.e.* $u(t) = K(s)\,(r(t) - y(t))$, and same weighting functions of section VI-A. Thus, the controller is given by

$$K(s) = 2.05 \cdot 10^{-4} \frac{(s+1752\omega_n)(s-0.8648\omega_n)(s+5.115\cdot 10^{-4}\omega_n)(s^2+0.02\omega_n s+\omega_n^2)}{(s+0.5313\omega_n)(s^2+3.2\cdot 10^{-4}\omega_n s+\omega_n^2)(s^2+1.352\omega_n s+1.628\omega_n^2)}.$$

This controller is then transformed into a phasor controller K_{cp} via Theorem 1 and applied according to the phasor-based architecture.

As in the previous cases, we apply an amplitude reference step at $t = 1\,\text{ms}$ and $\omega_0 = \omega_n$. The simulation results for the direct approach and of the ideal CPRM one are presented in Fig. 13. We observe that the behavior of both approaches are very similar to the results of section VI-A. This is justified by the use of the same weighting functions.

Now, we use K_{cp} in a phasor architecture with nonideal s2cp with $\omega_c = 2\pi \cdot 100\,\text{rad}\,\text{s}^{-1}$, obtaining the results presented in Fig. 14. As previously, we observe a similar performance degradation since the nonidealities of the synchronous demodulation are not taken into account explicitly for the control design.

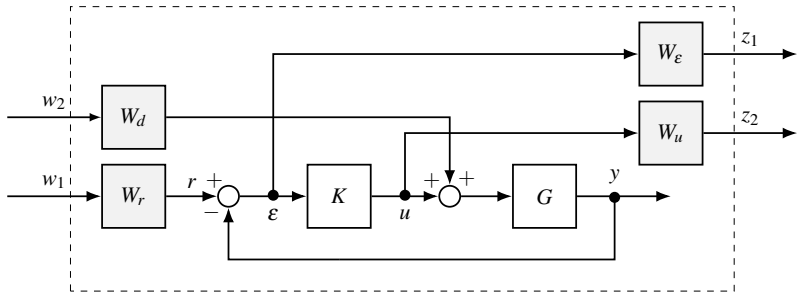

Fig. 12. H_∞ criterion for study case 3.

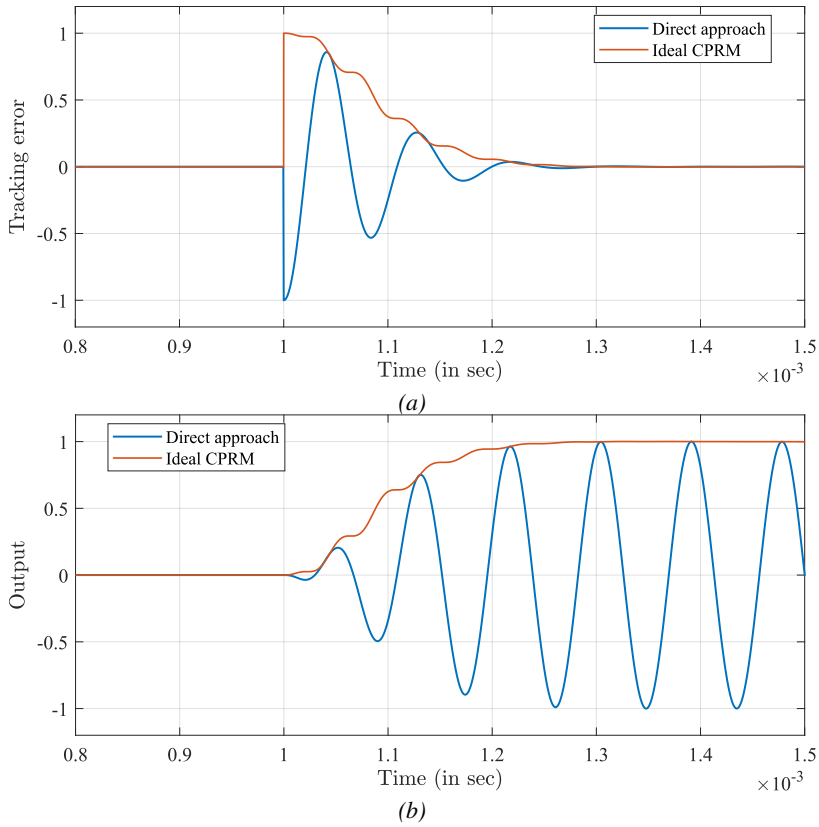

Fig. 13. Study case 3 - comparison between direct approach (G, K) and ideal CPRM (G_{cp}, K_{cp}).

To better investigate the effects of the nonideal s2cp in this example, [12] proposes special multipliers to describe the time-varying matrix $\Delta(\omega_0)$. In the referenced work, a stability analysis of the interconnection of $T_{n_{cp}\to y_{cp}}$ and $\Delta(\omega_0)$ is performed.

VII. Conclusions

In some applications, from the implementation point of view, it can be interesting to consider a phasor-based control architecture, as in MEMS sensors or electrical systems, for instance. However, this strategy includes several nonlinear elements into the control loop, what can make the control design a difficult task. In this paper, we have presented the complex phasor modeling, that allows to consider the to-be-controlled system as linear for the controller design.

Correspondences between classical control architectures and phasor-based ones were established. These equivalences allow one to design a linear controller in classical architecture and implement an equivalent controller in a phasor-based architecture, ensuring, in theory and at most, the same performances if the s2cp block is ideal. In practical implementations, nonidealities appear and can quickly degrade the performance of the closed-loop

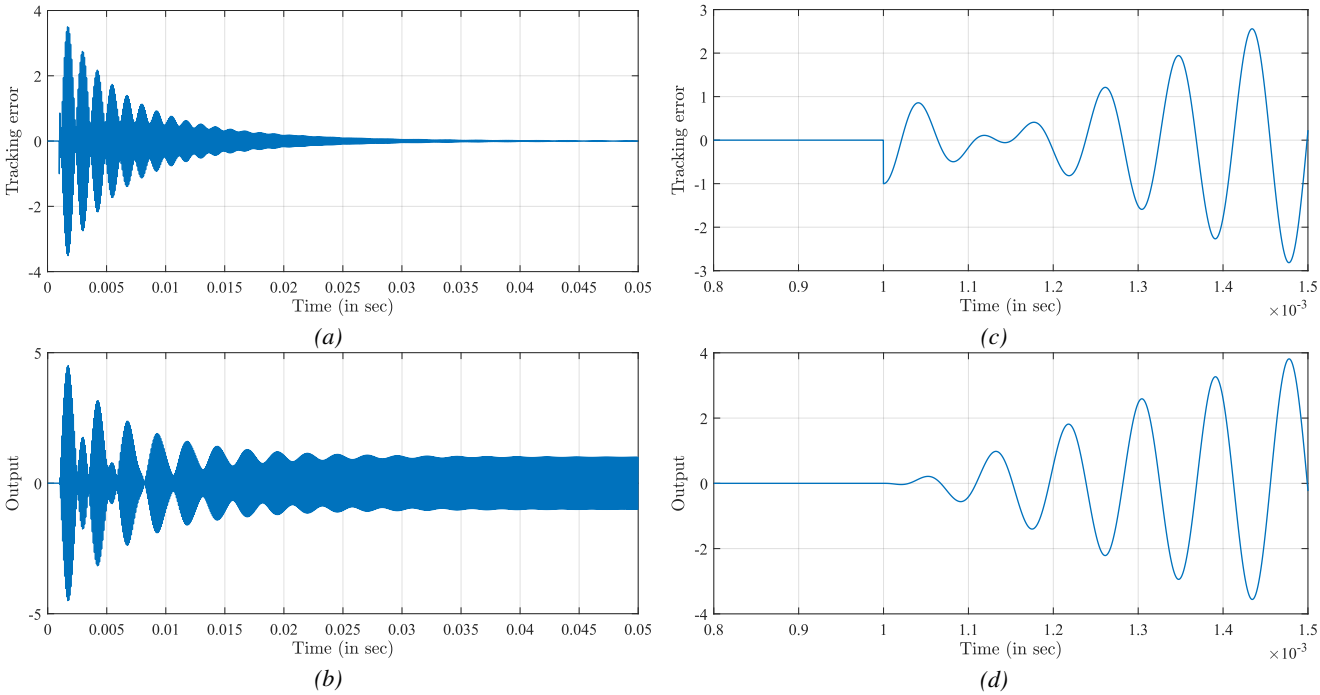

Fig. 14. Study case 3 - CPRM (G_{cp}, K_{cp}) with nonideal s2cp and $\omega_c = 2\pi 100\,\mathrm{rad\,s^{-1}}$. *(a)* tracking error and *(b)* output in a long time scale; zoom of *(c)* tracking error and *(d)* output.

system. The modeling of these nonidealities allows to analyze the closed-loop system and to take them into account to design a controller. Simulation results emphasized the effectiveness of the proposed method.

The final message of this paper is that if there are practical constraints imposing the use of a phasor architecture, the nonidealities of the s2cp block have to be taken into consideration, guaranteeing that the design specifications are verified in the real implementation.

References

[1] M. Saukoski, "System and circuit design for a capacitive MEMS gyroscope," Ph.D. dissertation, Helsinki University of Technology, 2008.

[2] V. Kempe, *Inertial MEMS - principles and practice*. Cambridge: Cambridge University Press, 2011.

[3] M. Egretzberger, F. Mair, and A. Kugi, "Model-based control concepts for vibratory MEMS gyroscopes," *Mechatronics*, vol. 22, no. 3, pp. 241–250, Apr. 2012.

[4] S. Skogestad and I. Postlethwaite, *Multivariable feedback control - analysis and design*, 2nd ed. John Wiley & Sons, 2001.

[5] G. Scorletti and L. E. Ghaoui, "Improved LMI conditions for gain scheduling and related control problems," *International Journal of Robust and Nonlinear Control: IFAC-Affiliated Journal*, vol. 8, no. 10, pp. 845–877, 1998.

[6] V. Venkatasubramanian, "Tools for dynamic analysis of the general large power system using time-varying phasors," *Int. J. Electr. Power Energy Syst.*, vol. 16, no. 6, pp. 365–376, 1994.

[7] K. Martin, "Complex signal processing is not complex," *IEEE Trans. Circuits Syst. I Regul. Pap.*, vol. 51, no. 9, pp. 1823–1836, 2004.

[8] O. Troeng, B. Bernhardsson, and C. Rivetta, "Complex-coefficient systems in control," in *2017 Am. Control Conf.*, no. 4. IEEE, may 2017, pp. 1721–1727.

[9] P. Gahinet, "Explicit controller formulas for LMI-based H_∞ synthesis," *Automatica*, vol. 32, no. 7, pp. 1007–1014, jul 1996.

[10] D. Vakman, "On the analytic signal, the Teager-Kaiser energy algorithm, and other methods for defining amplitude and frequency," *IEEE Trans. Signal Process.*, vol. 44, no. 4, pp. 791–797, apr 1996.

[11] B. Picinbono, "On instantaneous amplitude and phase of signals," *IEEE Trans. Signal Process.*, vol. 45, no. 3, pp. 552–560, 1997.

[12] J. Ayala-Cuevas, F. Saggin, G. Scorletti, and A. Korniienko, "Stability Analysis of Time-Varying Systems with Harmonic Oscillations Using IQC Frequency Domain Multipliers," 2019, (submitted to IEEE Int. Conf. Decis. Control).

[13] M. Vidyasagar, *Nonlinear systems analysis*, 2nd ed. Englewood Cliffs, NJ: Prentice Hall, 2002.

APPENDIX

A. Proof of the Property 3 (Theorem 3)

Proof. Please note that, by Theorem 2, the existence of a controller K such that $\|P\star K\|_\infty<\gamma$ is equivalent to the existence of the matrices $R=R^T$ and $S=S^T$ such that

$$\left[\diamond\right]_\perp^T \begin{bmatrix} SA_P^T+A_PS & B_w & SC_z^T \\ B_w^T & -\gamma I & D_{zw}^T \\ C_zS & D_{zw} & -\gamma I \end{bmatrix} \begin{bmatrix} B_u^T & 0 & D_{zu}^T \end{bmatrix}_\perp \prec 0, \tag{13}$$

$$\left[\diamond\right]_\perp^T \begin{bmatrix} A_P^TR+RA_P & RB_w & C_z^T \\ B_w^TR & -\gamma I & D_{zw}^T \\ C_z & D_{zw} & -\gamma I \end{bmatrix} \begin{bmatrix} C_y & D_{yw} & 0 \end{bmatrix}_\perp \prec 0 \tag{14}$$

$$\text{and} \quad \begin{bmatrix} R & I \\ I & S \end{bmatrix} \succ 0. \tag{15}$$

In its turn, again by Theorem 2, the existence of $\underset{\sim}{K}$ such that $\|P_{cp}\star\underset{\sim}{K}\|_\infty<\gamma$ is equivalent to the existence of matrices $\underset{\sim}{R}=\underset{\sim}{R}^T$ and $\underset{\sim}{S}=\underset{\sim}{S}^T$ such that

$$\left[\diamond\right]_\perp^T \begin{bmatrix} \underset{\sim}{S}A_{P_{cp}}^T+A_{P_{cp}}\underset{\sim}{S} & B_{w_{cp}} & \underset{\sim}{S}C_{z_{cp}}^T \\ B_{w_{cp}}^T & -\gamma I & D_{zw_{cp}}^T \\ C_{z_{cp}}\underset{\sim}{S} & D_{zw_{cp}} & -\gamma I \end{bmatrix} \begin{bmatrix} B_{u_{cp}}^T & 0 & D_{zu_{cp}}^T \end{bmatrix}_\perp \prec 0, \tag{16}$$

$$\left[\diamond\right]_\perp^T \begin{bmatrix} A_{P_{cp}}^T\underset{\sim}{R}+\underset{\sim}{R}A_{P_{cp}} & \underset{\sim}{R}B_{w_{cp}} & C_{z_{cp}}^T \\ B_{w_{cp}}^T\underset{\sim}{R} & -\gamma I & D_{zw_{cp}}^T \\ C_{z_{cp}} & D_{zw_{cp}} & -\gamma I \end{bmatrix} \begin{bmatrix} C_{y_{cp}} & D_{yw_{cp}} & 0 \end{bmatrix}_\perp \prec 0 \tag{17}$$

$$\text{and} \quad \begin{bmatrix} \underset{\sim}{R} & I \\ I & \underset{\sim}{S} \end{bmatrix} \succ 0. \tag{18}$$

For completeness, we recall that

$$\left[\begin{array}{c|c|c} A_{P_{cp}} & B_{u_{cp}} & B_{w_{cp}} \\ \hline C_{y_{cp}} & 0 & D_{yw_{cp}} \\ \hline C_{z_{cp}} & D_{zu_{cp}} & D_{zw_{cp}} \end{array}\right] = \left[\begin{array}{cc|cc|cc} A_P & \omega_0 I & B_u & 0 & B_w & 0 \\ -\omega_0 I & A_P & 0 & B_u & 0 & B_w \\ \hline C_y & 0 & 0 & 0 & D_{yw} & 0 \\ 0 & C_y & 0 & 0 & 0 & D_{yw} \\ \hline C_z & 0 & D_{zu} & 0 & D_{zw} & 0 \\ 0 & C_z & 0 & D_{zu} & 0 & D_{zw} \end{array}\right].$$

(Sufficient part: $K\Rightarrow\underset{\sim}{K}$) Let us assume that there exists K such that $\|P\star K\|_\infty<\gamma$. Then, we take the solutions of (13), (14) and (15) and build the matrices $\underset{\sim}{S}=\operatorname{diag}(S,S)$ and $\underset{\sim}{R}=\operatorname{diag}(R,R)$. These matrices are solution of (16), (17) and (18) since, after developing (16) and (17) the dependencies on ω_0 are canceled out, and we end up with the equations (13)–(15) repeated in a block diagonal structure.

(Necessary part: $\underset{\sim}{K}\Rightarrow K$) Now, assume that there exists $\underset{\sim}{K}$ such that $\|P_{cp}\star\underset{\sim}{K}\|_\infty<\gamma$. By partitioning

$$\underset{\sim}{S}=\begin{bmatrix} S_1 & S_2 \\ S_2^T & S_3 \end{bmatrix},$$

the inequality (16) can be rewritten as

$$\mathscr{N}^T \left[\begin{array}{cc|cc|cc} \Pi_{S1} & \Pi_{S2} & B_w & 0 & S_1C_z^T & S_2C_z^T \\ \Pi_{S2}^T & \Pi_{S3} & 0 & B_w & S_2^TC_z^T & S_3C_z^T \\ \hline B_w^T & 0 & -\gamma I & 0 & D_{zw}^T & 0 \\ 0 & B_w^T & 0 & -\gamma I & 0 & D_{zw}^T \\ \hline C_zS_1 & C_zS_2 & D_{zw} & 0 & -\gamma I & 0 \\ C_zS_2^T & C_zS_3 & 0 & D_{zw} & 0 & -\gamma I \end{array}\right] \mathscr{N} \prec 0 \tag{19}$$

with

$$\begin{aligned} \Pi_{S1} &= A_PS_1 + S_1{A_P}^T + \omega_0(S_2 + S_2^T) \\ \Pi_{S2} &= A_PS_2 + S_2{A_P}^T + \omega_0(-S_1 + S_3) \\ \Pi_{S3} &= A_PS_3 + S_3{A_P}^T - \omega_0(S_2 + S_2^T) \\ \mathscr{N} &= \begin{bmatrix} B_u^T & 0 & 0 & 0 & D_{zu}^T & 0 \\ 0 & B_u^T & 0 & 0 & 0 & D_{zu}^T \end{bmatrix}_\perp . \end{aligned}$$

Then, by permuting the lines and columns of (19), it is rewritten as

$$\begin{bmatrix} \mathscr{N}_B^T M_{S1} \mathscr{N}_B & \mathscr{N}_B^T M_{S2} \mathscr{N}_B \\ \mathscr{N}_B^T M_{S2}^T \mathscr{N}_B & \mathscr{N}_B^T M_{S3} \mathscr{N}_B \end{bmatrix} \prec 0 \tag{20}$$

with

$$\begin{aligned} \mathscr{N}_B &= \begin{bmatrix} B_u^T & 0 & D_{zu}^T \end{bmatrix}_\perp \\ M_{S1} &= \begin{bmatrix} \Pi_{S1} & B_w & S_1C_z^T \\ B_w^T & -\gamma I & D_{zw}^T \\ C_zS_1 & D_{zw} & -\gamma I \end{bmatrix} \\ M_{S2} &= \begin{bmatrix} \Pi_{S2} & 0 & S_2C_z^T \\ 0 & 0 & 0 \\ C_zS_2 & 0 & 0 \end{bmatrix} \\ M_{S3} &= \begin{bmatrix} \Pi_{S3} & B_w & S_3C_z^T \\ B_w^T & -\gamma I & D_{zw}^T \\ C_zS_3 & D_{zw} & -\gamma I \end{bmatrix} . \end{aligned}$$

Since the matrix of (20) is negative definite, the sum of its main diagonal blocks is also negative definite, *i.e.*,

$$\mathscr{N}_B^T \left(M_{S1} + M_{S3}\right) \mathscr{N}_B \prec 0.$$

Then, let us introduce $\widetilde{M}_S = \frac{1}{2}\left(M_{S1} + M_{S3}\right)$ and apply the same procedure to (17) and (18). We obtain

$$\mathscr{N}_B^T \widetilde{M}_S \mathscr{N}_B \prec 0$$

$$\mathscr{N}_C^T \widetilde{M}_R \mathscr{N}_C \prec 0$$

$$\begin{bmatrix} \widetilde{R} & I \\ I & \widetilde{S} \end{bmatrix} \succ 0$$

with

$$
\begin{aligned}
\mathcal{N}_C &= \begin{bmatrix} C_y & D_{yw} & 0 \end{bmatrix}_\perp \\
\widetilde{R} &= \tfrac{1}{2}\left(R_1 + R_3\right) \\
\widetilde{S} &= \tfrac{1}{2}\left(S_1 + S_3\right) \\
\widetilde{M}_R &= \begin{bmatrix} A_P^T\widetilde{R} + \widetilde{R}A_P & \widetilde{R}B_w & C_z^T \\ B_w^T\widetilde{R} & -\gamma I & D_{zw}^T \\ C_z & D_{zw} & -\gamma I \end{bmatrix} \\
\widetilde{M}_S &= \begin{bmatrix} \widetilde{S}A_P^T + A_P\widetilde{S} & B_w & \widetilde{S}C_z^T \\ B_w^T & -\gamma I & D_{zw}^T \\ C_z\widetilde{S} & D_{zw} & -\gamma I \end{bmatrix}
\end{aligned}
$$

This means that $\widetilde{R}$ and $\widetilde{S}$ are solution of the inequalities (13)–(15) of Theorem 2. Hence, this theorem ensures that there exists a controller K for P defined in (8), such that $\|P \star K\|_\infty < \gamma$. $\square$